

# Theoretical Modelling and Investigation of System Parameters of Organic Rankine Cycle with Nanofluid Used Solar Parabolic Trough Collector

Erhan Kirtepe<sup>1,\*</sup>, Oğuz Emrah Turgut<sup>2</sup>

<sup>1</sup> Department of Motor Vehicles and Transportation Technologies, Şırnak University, Şırnak, Turkey

<sup>2</sup> Department of Industrial Engineering, Bakırçay University, Izmir, Turkey

Received: 17.04.2021; Accepted: 28.06.2021; Published: 15.07.2021

Turk. J. Mater. Vol: 6 No: 1 Page: 9-18 (2021) ISSN: 2636-8668

SLOI: <http://www.sloi.org/sloi-name-of-this-article>

\*Correspondence E-mail: [erhan.kirtepe@sirnak.edu.tr](mailto:erhan.kirtepe@sirnak.edu.tr)

**ABSTRACT** In this study, theoretical modelling of Organic Rankine Cycle integrated with solar parabolic trough collector has been made. The validity of the theoretical model has been proved by comparing the model outcomes with the experimental results collected from in the literature work. The effect of adding nanoparticles ( $Al_2O_3$ , CuO, Cu,  $SiO_2$ ,  $TiO_2$ ) of different types and concentrations to the heat transfer fluid (Therminol VP-1, Syltherm 800) used in the PTC and using different refrigerants (Toluene, MDM, cyclohexane, n-pentane, n-Hexane, R11, R123, R113, R141b) in ORC on the system efficiency and performance have been investigated. The highest system efficiency is found to be 17.7% when Therminol VP-1 is chosen as the heat transfer fluid, Cu as the nanoparticle, and Toluene as the refrigerant.

**Keywords:** Solar energy, solar parabolic trough collector, Organic Rankine Cycle, nanofluid.

**Cite this article:** E. Kirtepe, O.E. Turgut. Theoretical Modelling and Investigation of System Parameters of Organic Rankine Cycle with Nanofluid Used Solar Parabolic Trough Collector. Turk. J. Mater. 6(1) (2021) 9-18.

## 1. INTRODUCTION

The increasing demand for energy worldwide, the environmental damage, and the depletion of fossil-based fuels has led to an increase in the need for renewable energy sources. Improving the performance of energy generation systems from renewable energy sources will enable us to benefit from these resources in the maximum amount. Many scientific research studies have been conducted on the effects of adding nanoparticles to different working fluids in thermal systems used to generate power from the solar energy resources. In addition, diligent efforts have been made on the influences of utilizing these systems integrated with other energy systems on the performance and efficiency of the system.

Abubakr et al. (2020) [1] performed energy and exergy optimization applying the Multi-Objective Genetic Algorithm (MOGA) to the parabolic trough solar collector (PTC) using nanofluid. In this study, Therminol VP-1, Syltherm 800, and Dowtherm Q were used as heat transfer fluids, and performance investigations were carried out by adding nanoparticles called  $Al_2O_3$ , CuO, and  $SiO_2$  different concentration ratios to these fluids. Risi et al. (2013) [2] examined the effects of adding nanoparticles (CuO and Ni) in the gas phase and different concentration ratios to the heat transfer fluid used in PTC on the thermal efficiency of PTC. In addition, they used Genetic Algorithm Optimization (MOGA II) to improve and optimize the performance of PTC. As a result of the analysis, the maximum thermal efficiency for PTC was found to be 62.5%. Ehyaei et al. (2019) [3] carried out energy, exergy, and economic analysis of PTC. The maximum exergy efficiency and minimum energy cost were simultaneously investigated by applying the Multi-Objective Swarm Optimization

(MOPSO) technique. According to the optimum results, exergy efficiency, energy efficiency, and heat cost are respectively 29.22%, 35.55%, and 0.0142 \$/kWh. Bellos and Tzivanidis (2017) [4] conducted the theoretical analysis of PTC working with ORC. They used Syltherm 800 as the heat transfer fluid and investigated the effect of adding different nanoparticles ( $\text{Al}_2\text{O}_3$ , CuO,  $\text{TiO}_2$ , Cu) to this fluid and assess the overall ORC system performance running with these different refrigerants (Toluene, MDM, cyclohexane, n-pentane). Moloodpoor et al. (2019) [5] developed a one-dimensional thermal model of PTC and proved the model's validity by comparing the model outcomes with the experimental results retrieved from the literature. In addition, they have optimized PTC using the IPSO (Integrated Particle Swarm Optimization) technique. Huang et al. (2016) [6] developed a 2-dimensional thermal model and a 3-dimensional optical model for PTC. The theoretical results calculated according to the developed numerical model were compared with those obtained from literature experimental studies and the validity of the model was proven. Alirahmi et al. [7] carried out the thermodynamic analysis, economic analysis, and multi-objective optimization of a system where hydrogen, freshwater, cooling load, and hot water are produced together using geothermal and solar energy. Coccia et al. (2016) [8] performed a numerical investigation over a PTC system. In the study, they used water-based nanofluids with different weight concentrations to increase the thermal efficiency of a PTC. They utilized different nanoparticles ( $\text{Fe}_2\text{O}_3$ ,  $\text{SiO}_2$ ,  $\text{TiO}_2$ , ZnO,  $\text{Al}_2\text{O}_3$ , and Au) in the analyzed nanofluids. The accuracy of the numerically calculated results has been proved by comparing the results of the experimental study using water as the heat transfer fluid. Mwesigye et al. (2016) [9] conducted a numerical study on the thermal and thermodynamic performance of PTC using Cu-Therminol VP-1 nanofluid as heat transfer fluid. Results showed that the thermal efficiency of PTC increases with the increasing nanoparticle volume fraction in the nanofluid solution.

In this study, theoretical modeling of an Organic Rankine Cycle (ORC) driven by Parabolic Trough Solar Collector (PTC-ORC) will be accomplished and numerically investigated. The accuracy of the theoretical model for PTC is validated by the experimental data obtained from the literature works. Incorporating nanoparticles ( $\text{Al}_2\text{O}_3$ , CuO, Cu,  $\text{SiO}_2$ ,  $\text{TiO}_2$ ) of different types and concentration into the working fluid used in PTC (Therminol VP-1, Syltherm 800) and the effects of using different refrigerants (Toluene, MDM, cyclohexane, n-pentane, n-Hexane, R11, R123, R113, R141b) in ORC on system efficiency and performance will be examined.

## 2. MATHEMATICAL MODEL

The schematic picture of the PTC-ORC system examined in this study is shown in Figure 1. As can be seen from this figure, thermal energy obtained from solar energy with PTC is transferred to the storage tank. The tank is filled with pure Therminol VP-1 fluid, and the total thermal energy from the collectors is transferred to the fluid in the tank through a heat exchange device. Through the heat transfer fluid circulating between the tank and the ORC, the thermal energy taken from the storage tank is exchanged with the refrigerant circulating in the ORC. Reaching high pressure and temperature in the evaporator of ORC, the refrigerant expands in the turbine and decreases to low pressure and temperature. Mechanical energy is generated with the expansion of the refrigerant in the turbine, and this mechanical energy is converted into electrical energy with a generator.

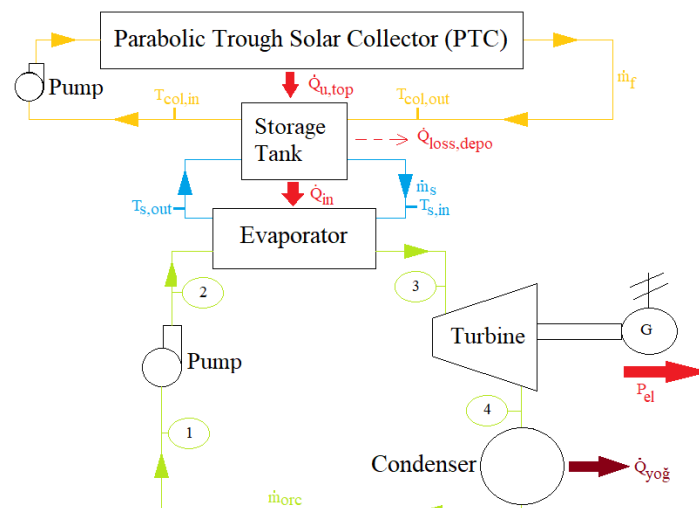


Figure 1. Schematic picture of the PTC-ORC system.

## 2.1 Parabolic trough solar collector

The radiation absorbed by the cylindrical receiver surface in the PTC depends on the optical properties of the PTC as well as on the effect of factors such as the geometric properties of the system components and the contamination resulting from the use. Estimates of effective optical efficiency terms are shown in Table 1.

Table 1. Estimates of effective optical efficiency terms [10]

Optical Efficiencies	Values
Heat Collector Element Shadowing (bellows, shielding, supports) ( $\gamma_1$ )	0,974
Tracking Error ( $\gamma_2$ )	0,994
Geometry Error (mirror alignment) ( $\gamma_3$ )	0,980
Dirt on Mirrors ( $\gamma_4$ )	0,995
Dirt on Heat Collector Element ( $\gamma_5$ )	0,997
Unaccounted ( $\gamma_6$ )	0,960
Clean Mirror Reflectance ( $\rho$ )	0,935

The solar radiation absorbed in the glass cover and the cylindrical receiving surface can be respectively expressed by Equations 1 and 2.

$$S_c = I_b \rho \left( \prod_{i=1}^6 \gamma_i \right) \alpha_c K \quad (1)$$

$$S_r = I_b \rho \left( \prod_{i=1}^6 \gamma_i \right) \tau_c \alpha_r K \quad (2)$$

The heat transfer between the glass cover and the external environment by convection and radiation is calculated by Equation 3.

$$Q_{c-a} = \varepsilon_c \pi D_{c,o} L \sigma (T_{c,o}^4 - T_{sky}^4) + h \pi D_{c,o} L (T_{c,o} - T_a) \quad (3)$$

The sky temperature here is calculated as a function of the outdoor air temperature as expressed in Equation 4 [11].

$$T_{sky} = 0.0552 T_a^{1.5} \quad (4)$$

The correlation proposed by McAdams (1954) is used to obtain the heat transfer coefficient between the glass cover and the environment [12].

$$Nu_{air} = 0,40 + 0,54 Re_{air}^{0,52} \quad 0,1 < Re_{air} < 1000 \quad (5)$$

$$Nu_{air} = 0,30 Re_{air}^{0,6} \quad 1000 < Re_{air} < 50000 \quad (6)$$

$$Re_{air} = \frac{\rho_{air} V_{wind} D_{c,o}}{\mu_{air}} \quad (7)$$

The thermodynamic properties of the air ( $\rho_{air}$  and  $\mu_{air}$ ) are calculated from the average temperature ( $T_{m,air}$ ) of the ambient air and the glass cover outer surface.

$$T_{m,air} = \frac{T_{c,o} + T_{air}}{2} \quad (8)$$

The heat transfer by conduction in the glass cover is obtained using Equation 9.

$$Q_c = \frac{2\pi k_c L (T_{c,i} - T_{c,o})}{\ln\left(\frac{D_{c,o}}{D_{c,i}}\right)} \quad (9)$$

The heat transfer between the inner surface of the glass cover and the cylindrical receiver's outer surface is determined using Equation 10. In this study, the  $k_{eff}$  value is taken as zero since it is assumed that there is a vacuum between the inner surface of the glass cover and the cylindrical receiver's outer surface.

$$Q_{c,i-r,o} = \frac{\pi D_{r,o} L \sigma (T_{r,o}^4 - T_{c,i}^4)}{\frac{1}{\varepsilon_r} + \frac{1 - \varepsilon_c}{\varepsilon_c} \left(\frac{D_{r,o}}{D_{c,i}}\right)} + \frac{2\pi k_{eff} L (T_{r,o} - T_{c,i})}{\ln \frac{D_{c,i}}{D_{r,o}}} \quad (10)$$

The outer surface of the cylindrical receiver is considered to be a cermet selective surface, and the emissivity of this surface can be obtained via Equation 11, which depends on the outer surface temperature of the cylindrical receiver [10].

$$\varepsilon_r = 0,000327 \times T_{r,o} - 0,06597 \quad (11)$$

The useful heat transferred to the heat transfer fluid in PTC is calculated from Equation 12 depending on the fluid inlet and ambient air temperature.

$$Q_u = A_a F_R \left[ S - \frac{A_r}{A_a} U_L (T_{f,i} - T_a) \right] \quad (12)$$

The collector heat removal factor ( $F_R$ ) can be found by Equation 13.

$$F_R = F'' \times F' \quad (13)$$

$F''$  and  $F'$  shown in Equation 13 are respectively collector flow factor and collector efficiency factor and calculated by Equations 14 and 15.

$$F'' = \frac{\dot{m} c_p}{A_r U_L F'} \left( 1 - \exp \left( - \frac{A_r U_L F'}{\dot{m} c_p} \right) \right) \quad (14)$$

$$F' = \frac{1/U_L}{\frac{1}{U_L} + \frac{D_{r,o}}{h_{f,i} D_{r,i}} + \frac{D_{r,o} \ln(D_{r,o}/D_{r,i})}{2k_r}} \quad (15)$$

If the flow regime of the heat transfer fluid is laminar ( $Re_{f,i} < 2300$ ), the Nusselt number between the cylindrical receiver's inner surface and the heat transfer fluid is 4.36 ( $Nu_{f,i} = 4.36$ ), and the corresponding friction factor is obtained by Eq. 16 [13].

$$f = 64/Re_{f,i} \quad (16)$$

If the flow regime of the heat transfer fluid is turbulent, the correlation proposed by Gnielinski is used to calculate the Nusselt number between the inner surface of the cylindrical receiver and the heat transfer fluid whose exact formulation is given by Equations 17 and 18. This equation is valid under  $0.5 \leq Pr \leq 2000$  and  $3 \times 10^3 < Re < 5 \times 10^6$  [13].

$$Nu_{f,i} = \frac{(f/8) (Re_w - 1000) Pr_{f,i}}{1 + 12.7 (f/8)^{0.5} (Pr_{f,i}^{2/3} - 1)} \quad (17)$$

$$f = (1.58 \ln Re_w - 3.28)^{-2} \quad (18)$$

## 2.2 Nanofluid Properties

In this study, two different base heat transfer fluids, Syltherm 800 and Therminol VP-1 are utilized in PTC. The nanoparticles' thermophysical properties ( $Al_2O_3$ , CuO,  $TiO_2$ , Cu,  $SiO_2$ ) incorporated into the base heat transfer fluid are shown in Table 2.

Table 2. Nanoparticles' properties [1, 4].

Nanoparticle	$\rho_{np}$ (kg/m <sup>3</sup> )	$k_{np}$ (W/mK)	$c_{p,np}$ (J/kgK)
$Al_2O_3$	3970	40	765
CuO	6320	77	532
$TiO_2$	4250	8.95	686
Cu	8933	401	385
$SiO_2$	3970	1.4	765

Thermal properties of nanofluids are obtained by using equations 19, 20, 21, and 22. Here, bf and np subscripts respectively symbolize the base fluid and the nanoparticle [4].

$$\rho_{nf} = \rho_{bf}(1 - \phi) + \rho_{np}\phi \quad (19)$$

$$c_{p,nf} = \frac{\rho_{bf}(1-\phi)}{\rho_{nf}} \cdot c_{p,bf} + \frac{\rho_{np}\phi}{\rho_{nf}} \cdot c_{p,np} \quad (20)$$

$$k_{nf} = k_{bf} \frac{k_{np} + 2k_{bf} + 2(k_{np} - k_{bf})(1 + \beta)^3 \phi}{k_{np} + 2k_{bf} - (k_{np} - k_{bf})(1 + \beta)^3 \phi} \quad (21)$$

The  $\beta$  is the ratio of the nanolayer thickness to the original particle radius, and when calculating the thermal conductivity of the nanofluids, it is generally taken equal to 0.1 [4].

$$\mu_{nf} = \mu_{bf}(1 + 2,5\phi + 6,5\phi^2) \quad (22)$$

### 2.3 Mathematical Model of ORC and Storage Tank

In the PTC, it is assumed that the useful heat extracted from the sun is wholly transferred to the storage tank in the steady-state analysis of the system. This is a reasonable conceptualization for the heat transfer model simulated at steady-state [4]. Equation 23 is used.

$$Q_{u,top} = (UA)_{col-st} \cdot \frac{(T_{col,out} - T_{col,in})}{\ln \left[ \frac{T_{col,out} - T_{st}}{T_{col,in} - T_{st}} \right]} \quad (23)$$

The temperature distribution of the fluid in the tank ( $T_{st}$ ) is assumed to be uniform, and the numerical value of  $(UA)_{col-st}$  is taken as 12 kW/m<sup>2</sup>K [4]. The general energy balance for the storage tank is given in Equation 24.

$$Q_{stored} = Q_{u,top} - Q_{loss,st} - \dot{m}_s c_{p,s} (T_{s,in} - T_{s,out}) \quad (24)$$

The amount of energy stored in the storage tank ( $Q_{stored}$ ) equals to zero for steady-state approximation. The heat loss from the storage tank to the outside environment is calculated by Equation 25.

$$Q_{loss,st} = U_{st} A_{st} (T_{st} - T_a) \quad (25)$$

The total heat loss coefficient ( $U_{st}$ ), which includes the heat loss from the storage tank to the environment, convection and conduction, is taken equal to 0.5 W/m<sup>2</sup>K [4]. The surface area of the storage tank is calculated by Equation 26.

$$A_{st} = \frac{\pi D_{st}^2}{2} + \pi D_{st} L_{st} \quad (26)$$

The heat imposed for the evaporation of the refrigerant in the ORC evaporation ( $Q_{in,orc}$ ) is calculated from Equation 27.

$$Q_{in,orc} = \dot{m}_s c_{p,s} (T_{s,in} - T_{s,out}) = \dot{m}_{orc} (h_3 - h_2) \quad (27)$$

In ORC, pressure ratio (PR) is defined as the ratio of high pressure ( $P_{max}$ ) to the critical pressure of the refrigerant used.

$$PR = \frac{P_{max}}{P_{cr}} \quad (28)$$

The isentropic efficiencies of the turbine and pump used in the ORC are respectively shown by Equations 29 and 30

$$\eta_{turb,orc} = \frac{h_3 - h_{4a}}{h_3 - h_{4s}} \quad (29)$$

$$\eta_{pump,orc} = \frac{w_{pump,s}}{w_{pump,a}} = \frac{h_{2s} - h_1}{h_{2a} - h_1} \quad (30)$$

The power required for the pump in isentropic and real conditions is calculated by using Equations 31 and 32, respectively.

$$w_{pump,s} = v_1 (P_2 - P_1) \quad (31)$$

$$w_{pump,a} = \frac{w_{pump,s}}{\eta_{pump}} = \frac{v_1 (P_2 - P_1)}{\eta_{pump}} \quad (32)$$

In ORC, the mechanical energy obtained from the turbine is converted into electrical energy through a generator. The electrical power obtained is determined using Equation 33.

$$P_{el} = \eta_{mg} \dot{m}_{orc} (h_3 - h_{4a}) \quad (33)$$

The net electrical power generation obtained in ORC and the efficiency of ORC are respectively calculated with Equations 34 and 35.

$$P_{net,orc} = P_{el} - W_{pump,orc} \quad (34)$$

$$\eta_{orc} = \frac{P_{net,orc}}{Q_{in,orc}} \quad (35)$$

The net electrical power generated in the PTC-ORC system and the thermodynamic efficiency of the system are acquired by using Equations 36 and 37.

$$P_{net,sys} = P_{el} - W_{pump,orc} - W_{pump,PTC} \quad (36)$$

$$\eta_{sys} = \frac{P_{net,sys}}{N[l_b(D_a - D_{c,o})]L} \quad (37)$$

The constant parameters of the PTC-ORC system used in the study are shown in Table 3.

Table 3. Constant parameters of the PTC-ORC system [4, 5, 14].

Parameters	Values	Parameters	Values
Ambient temperature ( $T_a$ )	25 °C	Absorber absorptance ( $\alpha_r$ )	0,96
Solar beam irradiation ( $I_b$ )	800 W/mK	Absorber thermal conductivity ( $k_r$ )	54 W/mK
Condenser temperature ( $T_{yog}$ )	40 °C	Cover outer diameter ( $D_{c,o}$ )	0.125 m
Storage tank bottom diameter ( $D_{st}$ )	2 m	Cover inner diameter ( $D_{c,i}$ )	0.120 m
Storage tank height ( $L_{st}$ )	3.2 m	Cover emittance ( $\epsilon_c$ )	0,90
Heat exchanger effectiveness ( $UA$ ) <sub>col-st</sub>	12 kW/m <sup>2</sup>	Cover transmittance ( $\tau_c$ )	0,95
Volumetric flow rate of heat transfer fluid in PTC ( $\dot{V}_f$ )	3 m <sup>3</sup> /h	Cover thermal conductivity ( $k_c$ )	1.2
Number of PTC modules ( $N$ )	30	Collector area	5x8 m <sup>2</sup>
PTC module length ( $L$ )	8 m	Wind speed ( $V$ )	1 m/s
Incident angle modifier ( $K$ )	1	Turbine isentropic efficiency ( $\eta_{turbine}$ )	0,85
Absorber outer diameter ( $D_{r,o}$ )	0.07 m	Pump isentropic efficiency ( $\eta_{pump}$ )	0,70
Absorber inner diameter ( $D_{r,i}$ )	0.066 m	Electromechanical efficiency of the generator ( $\eta_{generator}$ )	0,98

### 3. VALIDITY OF THE THEORETICAL MODEL FOR PTC

In this study, the validity of the theoretical model developed for PTC is proven by comparing model outcomes with those obtained for the experimental studies carried out in Sandia National Laboratory [14]. In the empirical study, Syltherm 800 is used as the heat transfer fluid in PTC, and the situation where there is a vacuum in the annular region between the cylindrical receiving surface and the glass cover has been investigated. The comparative results are reported in Table 4. Between the developed theoretical model and the experimental results, the maximum uncertainty according to the outlet temperature of the fluid from the collector and the PTC efficiency is 1.23 °C and 2.82%, respectively.

Table 4. Comparison of the theoretical model developed in this study with the experimental results.

Case	$I_b$ (W/m <sup>2</sup> )	Wind speed (m/s)	$T_a$ (°C)	Flow rate (L/d)	Syltherm 800 inlet (°C)	Syltherm 800 outlet (°C)		Experiment Error (°C)	Thermal Efficiency (%)		Thermal Efficiency Error(%)	
						Exp.	Model		Exp.	Model	Exp.	Model
1	933,7	2,6	21,2	47,7	102,2	124,0	122,95	1,05	72,51	69,91	1,95	2,60
2	968,2	3,7	22,4	47,8	151,0	173,3	172,74	0,56	70,90	70,42	1,92	0,48
3	982,3	2,5	24,3	49,1	197,5	219,5	219,04	0,46	70,17	69,85	1,81	0,32
4	909,5	3,3	26,2	54,7	250,7	269,4	268,77	0,63	70,25	68,87	1,90	1,38
5	937,9	1,0	28,8	55,5	297,8	316,9	316,08	0,82	67,98	66,37	1,86	1,61
6	880,6	2,9	27,5	55,6	299,0	317,2	316,10	1,10	68,92	66,17	2,06	2,75
7	920,9	2,6	29,5	56,8	379,5	398,0	396,77	1,23	62,34	59,52	2,41	2,82
8	903,2	4,2	31,1	56,3	355,9	374,0	373,02	0,98	63,82	61,62	2,36	2,20

#### 4. RESULTS AND DISCUSSION

After proving the validity of the theoretical model developed for PTC by comparing it with the experimental results in the literature, the theoretically optimum system parameters of the PTC-ORC system, whose fixed parameters are given in Table 3, have been examined. Firstly, the effect of using Syltherm 800 and Therminol VP-1 fluids in PTC on the thermal performance of PTC is examined. As seen in Figure 2, the use of Therminol VP-1 as a heat transfer fluid increases the thermal performance. For this reason, Therminol VP-1 is chosen as the main heat transfer fluid used in PTC in the other analyses conducted within the scope of the study.

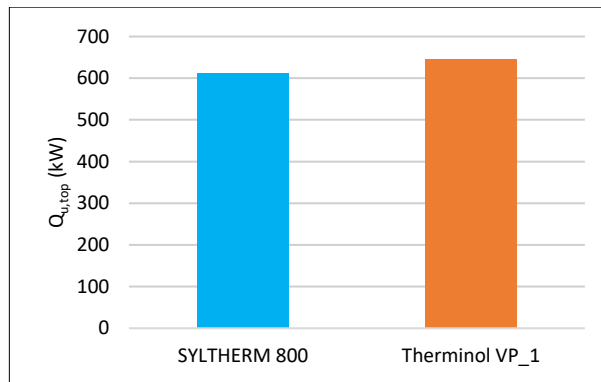


Figure 2. Effect of using Syltherm 800 and Therminol VP-1 on thermal performance in PTC.

After the selection of the base heat transfer fluid, it is investigated which nanoparticle should be incorporated into the base fluid. For this reason, as shown in Figure 3, the effect of five different nanoparticles ( $\text{Al}_2\text{O}_3$ , CuO, Cu,  $\text{SiO}_2$ ,  $\text{TiO}_2$ ) with different concentration ratios on the thermal efficiency of PTC is examined. The concentration ratio being zero indicates the pure state of the heat transfer fluid. As a result of the analysis, it is shown that increasing the concentration ratio positively affects the efficiency. Between them, the best thermal efficiency is obtained by using Cu as the nanoparticle.

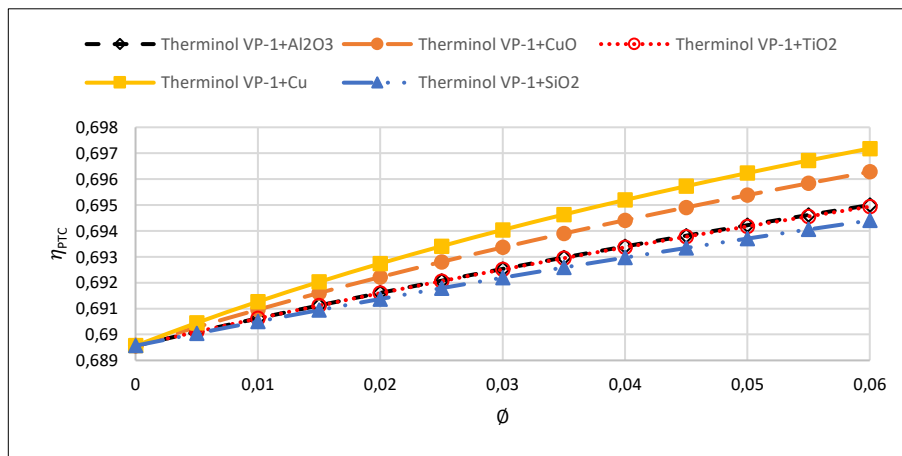


Figure 3. The effect of concentration ratios of different nanoparticles on PTC efficiency.

Different refrigerants (Toluene, MDM, cyclohexane, n-pentane, n-Hexane, R11, R123, R113, R141b) are used in the ORC system, and the effect of these refrigerants on the ORC efficiency is investigated. As a result of the theoretical analyses and as seen in Figure 4, the highest ORC efficiency is obtained when Toluene is used as the running refrigerant.

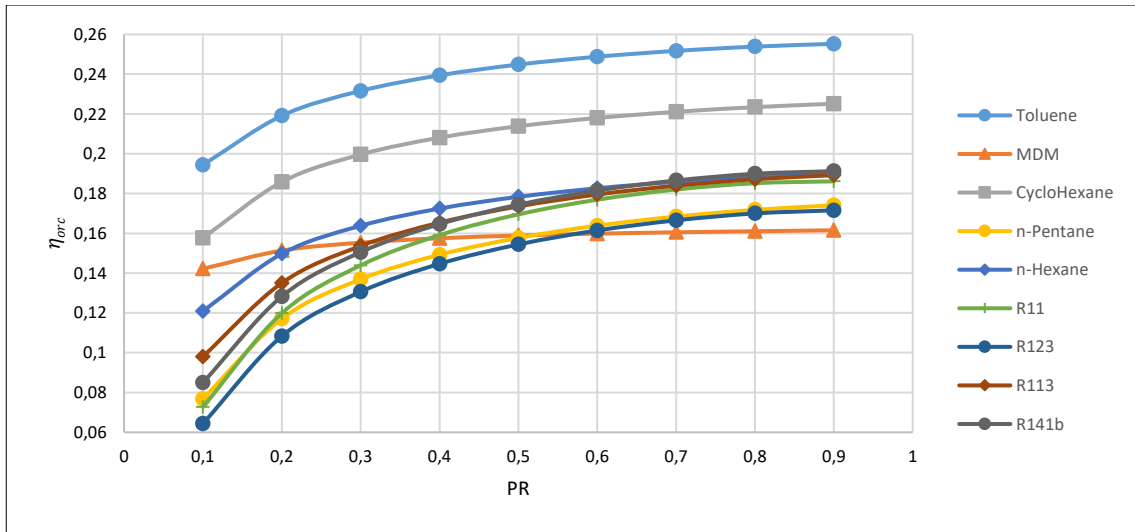


Figure 4. The effect of different refrigerants and different pressure ratios on ORC efficiency.

In the case of Therminol VP-1 as the base heat transfer fluid in PTC, Cu as a nanoparticle, and Toluene as the ORC refrigerant, its performance from the system has been investigated. As a result of the analyses made under the specified conditions, the change of the net electrical power obtained from the system and the system efficiency depending on the changing nanoparticle concentration ratio and pressure ratio can be seen in Figures 5 and 6. As a result of the analyses made under the specified conditions, the highest electrical power and system efficiency was 165,652 kW and 17.7%, respectively.

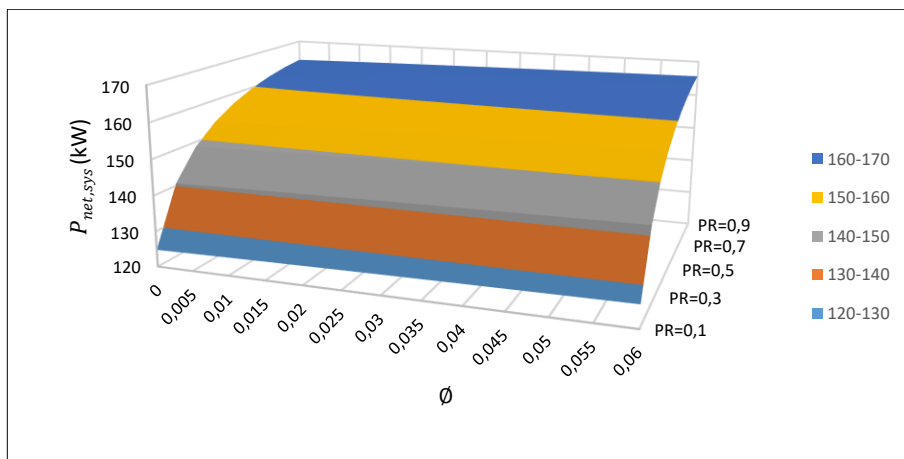


Figure 5. The variation of the net electrical power obtained from the system with the nanoparticle concentration and pressure ratio.

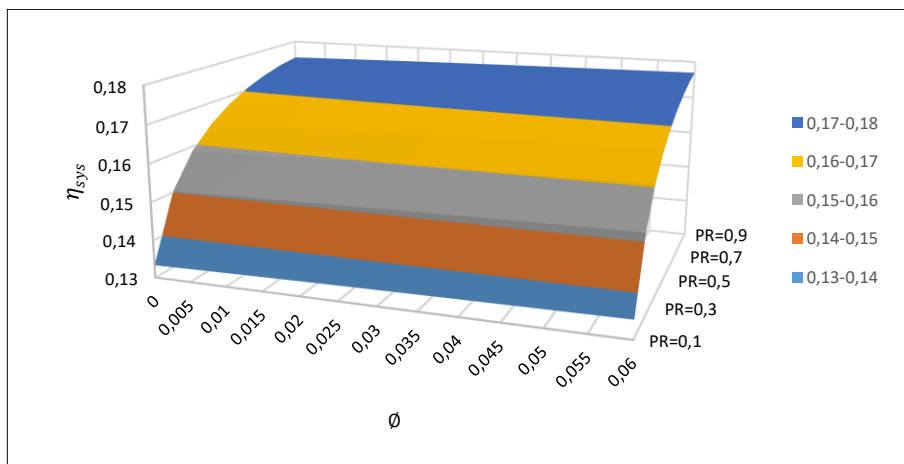


Figure 6. Variation of system efficiency with nanoparticle concentration and pressure ratio.

## 5. CONCLUSIONS

In this study, the effect of adding different nanoparticles ( $\text{Al}_2\text{O}_3$ ,  $\text{CuO}$ ,  $\text{Cu}$ ,  $\text{SiO}_2$ ,  $\text{TiO}_2$ ) to various heat transfer fluids (Syltherm 800, Therminol VP-1) in PTC on the thermal performance of PTC was investigated. In addition, the effect of using different refrigerants in ORC on cycle efficiency has been investigated. After selecting the appropriate nanofluid and refrigerant, the variations of PTC-ORC system efficiency with the pressure ratio and nanoparticle concentration ratio is examined, and the highest efficiency of the system is found to be 17.7%. In the future studies, system efficiency can be increased by trying such integrated applications. In addition, system performances can be improved by examining different nanofluids and refrigerants.

## REFERENCES

- [1] Abubakr, M., Amein, H., Akoush, B.M., El-Bakry, M.M. & Hassan, M.A., An intuitive framework for optimizing energetic and exergetic performances of parabolic trough solar collectors operating with nanofluids, *Renewable Energy*, **157**, 130-149, 2020.
- [2] Risi, A., Milanese, M. & Laforgia, D., Modelling and optimization of transparent parabolic trough collector based on gas-phase nanofluids, *Renewable Energy*, **58**, 134-139, 2013.
- [3] Ehyaei, M.A., Ahmadi, A., El Haj Assad, M. & Salameh, T., Optimization of parabolic through collector (PTC) with multi objective swarm optimization (MOPSO) and energy, exergy and economic analyses, *Journal of Cleaner Production*, **234**, 285-296, 2019.
- [4] Bellos, E. & Tzivanidis, C., Parametric analysis and optimization of an Organic Rankine Cycle with nanofluid based solar parabolic trough collectors, *Renewable Energy*, **114**, 1376-1393, 2017.
- [5] Moloodpoora, M., Mortazavib, A. & Ozbalta, N., Thermal analysis of parabolic trough collectors via a swarm intelligence optimizer, *Solar Energy*, **181**, 264-275, 2019.
- [6] Huang, W., Xu, Q. & Hu, P., Coupling 2D thermal and 3D optical model for performance prediction of a parabolic trough solar collector, *Solar Energy*, **139**, 365-380, 2016.
- [7] Alirahmi, S.M., Rostami, M. & Farajollahi, A.H., Multi-criteria design optimization and thermodynamic analysis of a novel multigeneration energy system for hydrogen, cooling, heating, power, and freshwater, *International journal of hydrogen energy*, **45**, 15047- 15062, 2020.
- [8] Coccia, G., Nicola, G.D., Colla, L., Fedele, L. & Scattolini, M., Adoption of nanofluids in low-enthalpy parabolic trough solar collectors: Numerical simulation of the yearly yield, *Energy Conversion and Management*, **118**, 306-319, 2016.
- [9] Mwesigye, A., Huan, Z. & Meyer, J.P., Thermal performance and entropy generation analysis of a high concentration ratio parabolic trough solar collector with Cu-Therminol VP-1 nanofluid, *Energy Conversion and Management*, **120**, 449-465, 2016.
- [10] Forristall R., Heat Transfer Analysis and Modelling of A Parabolic Trough Solar Receiver Implemented in Engineering Equation Solver, *NREL/TP-550-34169*, 2003.
- [11] Kırtepe, E., Yılmaz, R. & Özbalta, N., Parabolik Yoğunlaştırıcı Toplayıcıların Teorik Modellenmesi ve Farklı Sistem Parametrelerinin Verime Etkisinin İncelenmesi, *22. Ulusal Isı Bilimi ve Tekniği Kongresi*, 781-790, 11-14 Eylül, 2019.
- [12] Duffie, J.A. & Beckman, W.A., Solar Engineering of Thermal Processes, 4<sup>th</sup> ed., *John Wiley and Sons.*, 2013.
- [13] Çengel, Y.A. & Ghajar, A.J., Isı ve Kütle Transferi, *Palme Yayıncılık*, 2015.
- [14] Dudley, V.E., Kolb, G.J., Mahoney, A.R., Mancini, T.R., Matthews, C.W., Sloan M. & Kearney D., Test Results: SEGS LS-2 Solar Collector, *Report of Sandia National Laboratories (SANDIA-94-1884)*, 1994.

***Acknowledgement: 5<sup>th</sup> International Anatolian Energy Symposium  
24-26 March 2021, Karadeniz Technical University, Trabzon/Turkey***